Mass meta-analysis in Talairach space

Finn Årup Nielsen

Neurobiology Research Unit, Rigshospitalet;
Informatics and Mathematical Modelling
Technical University of Denmark

December 9, 2004

Elements for neuroinformatics data mining

Human brain mapping experiments represented by their Talairach coordinates in the Brede Database.

Labeling of experiments based on a simple ontology.

Construction of multiple volumes by simple kernel density estimation.

Permutation maximum statistics.

Modeling of the permutation distribution by a nonlinear model.

Reporting of the most consistent results.

Human brain mapping

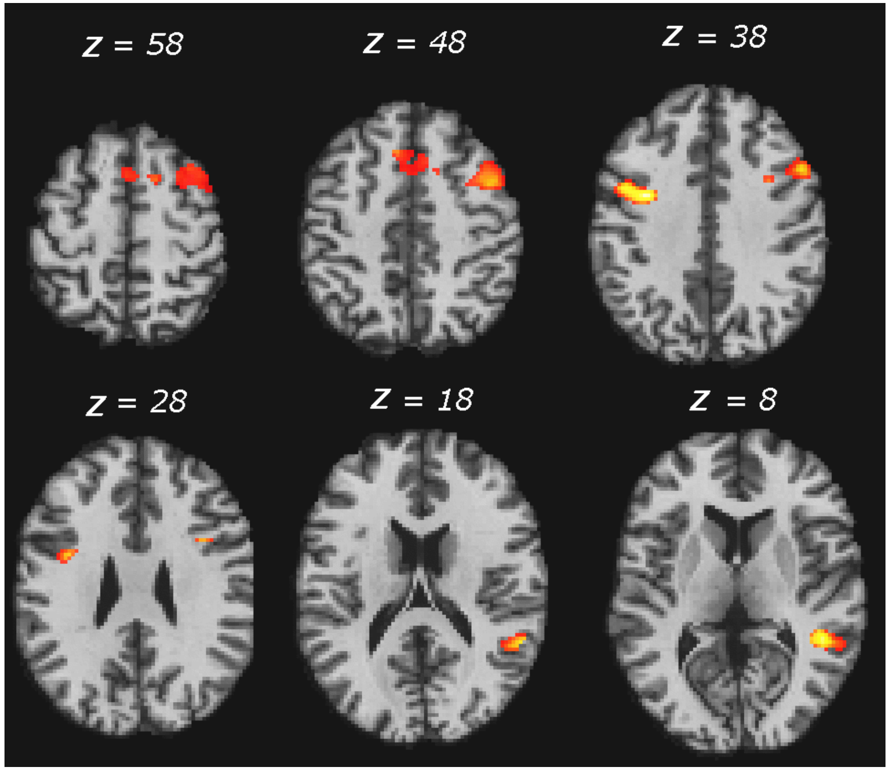

Figure 1: Results from a human brain mapping study (Balslev et al., 2004, figure 2).

PET or fMRI brain scans of the human brain while subjects are engaged in different mental processes.

Result represented in the literature with lists of three dimensional coordinates (in standardized "Talairach" brain space) (Talairach and Tournoux, 1988) of the hot spot activations, e.g.,

(x, y, z)	z-score
$-38, 0, 40$	4.91
$48, -42, 8$	4.66
$52, 14, 38$	4.07

Brede Database

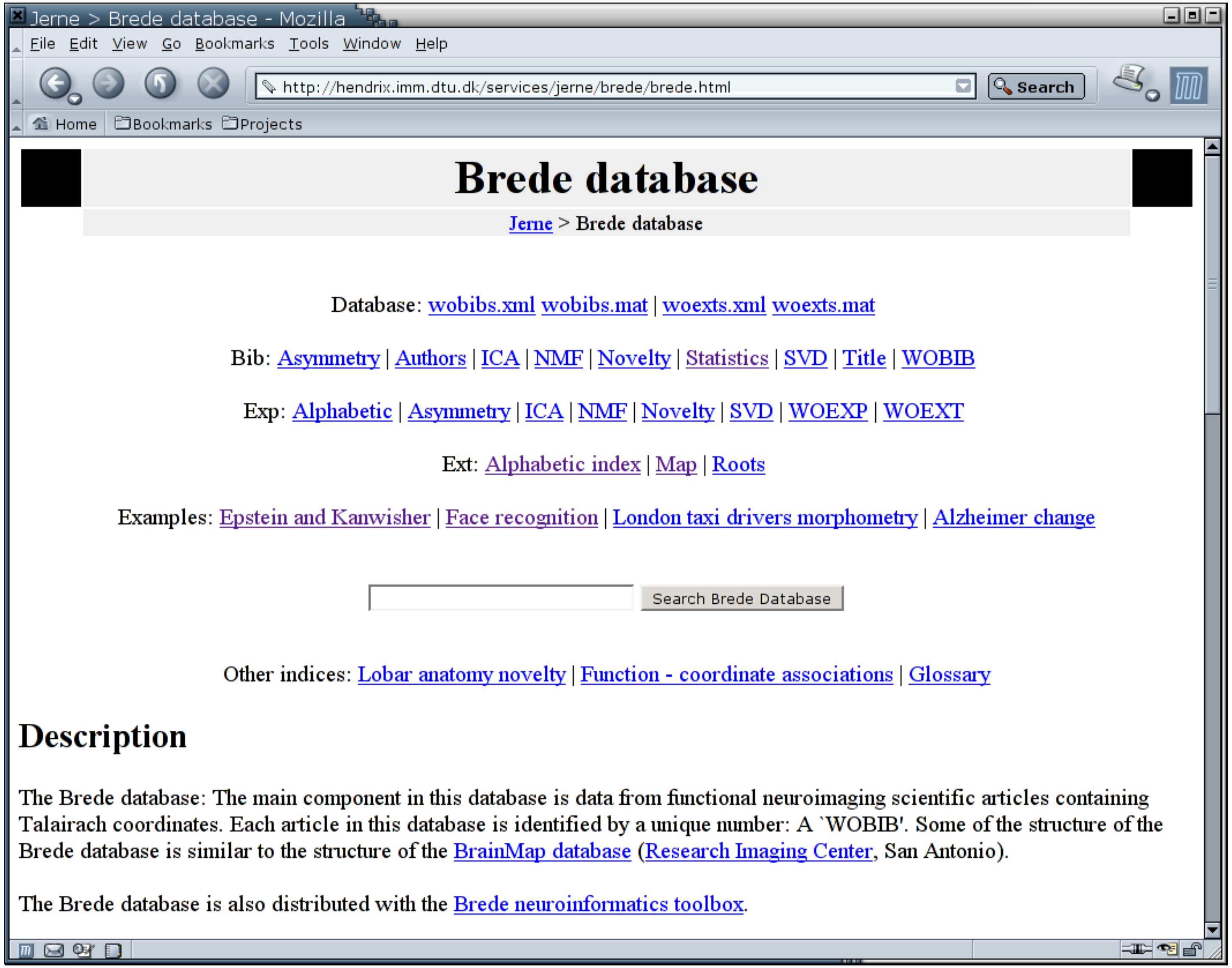

The Brede Database contains human brain mapping experiments reporting coordinates in Talairach space (Nielsen, 2003).

Presently information from 143 papers, containing 439 experiments and 3083 Talairach coordinates.

Bibliographic details, experimental details, Talairach coordinates.

Experiments organized in a simple ontology.

XML (and .mat Matlab) files available on the web with complete database.

WOEXP: 390 - Increased benzodiazepine receptor binding in panic disorder

Bib -> Asymmetry | Author | ICA | NMF | Novelty | Statistics | SVD | Title | WOBIB]

Exp -> Alphabetic | Asymmetry | ICA | NMF | Novelty | SVD | WOEXP | WOEXT]

Ext -> Alphabetic index | Map | Roots]   [Brede]   Loc -> Statistics]

[WOEXP_390] **Increased benzodiazepine receptor binding in panic disorder**. *Increased benzodiazepine receptor binding in panic disorder in panic disorder patients versus normal control subjects.* WOEXP: 390.

J. D. Bremner; R. B. Innis; T. White; M. Fujita; D. Silbersweig; A. W. Goddard; L. Staib; E. Stern; A. Cappiello; S. Woods; R. Baldwin; D. S. Charney. *SPECT [I-123]iomazenil measurement of the benzodiazepine receptor in panic disorder.*. *Biol Psychiatry* **47**(2):96-106, 2000. PMID: 10664825. WOBIB: 126.

Disease - Panic disorder
WOEXT: 234.
WOEXT: 380.

Modality:	SPECT/MRI
Measured variable:	Distribution volume
Tracer:	I-123 Iomazenil
Scanner:	Digital Scintigraphics CERASPECT
Number of subjects:	29

Asymmetry: -0.27344 (left: -1, right: +1)

x	y	z	Lobar anatomy	Functional area	WOROI	Value
-16	-1	18	Right caudate			
-18	-75	18	Cuneus (occipital cortex)			
34	29	28	Right middle frontal gyrus			

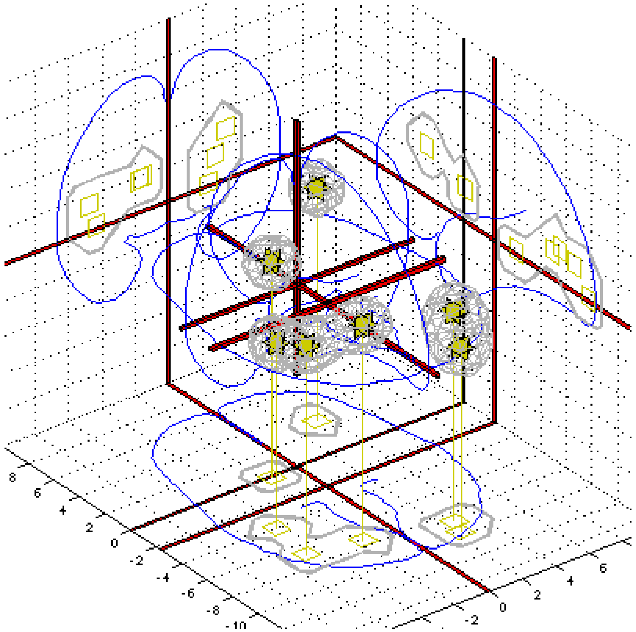

[PNG | VRML (87Kb)]

External components

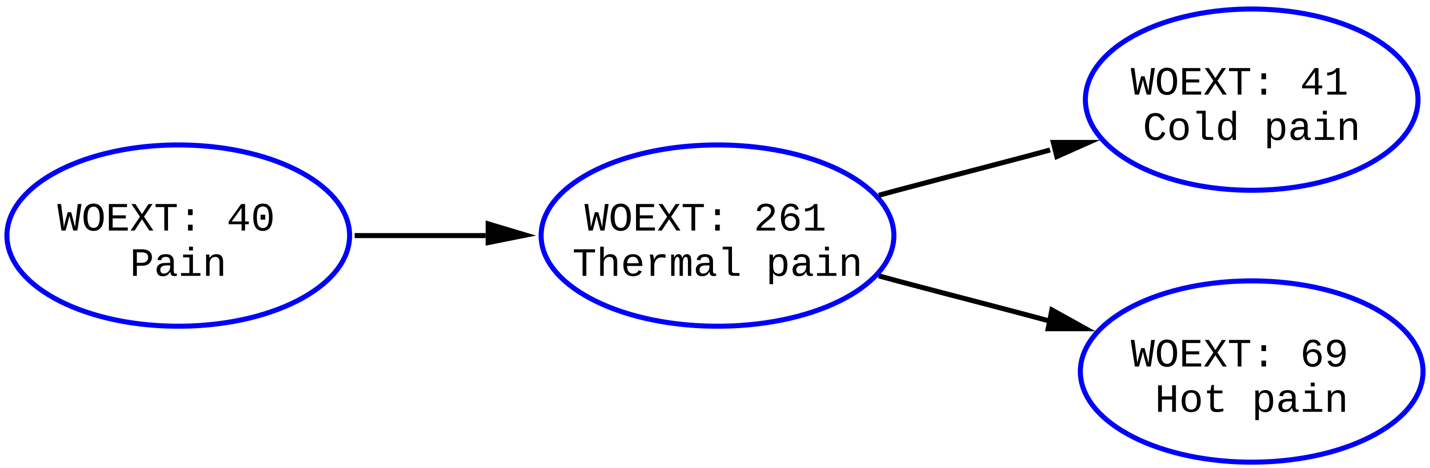

Figure 2: The external components around "thermal pain" with "pain" as the parent of "thermal pain" and "cold pain" and "hot pain" as children. Four components of a total of presently 460.

Experiments in the Brede Database are labeled with items from a taxonomy (a simple ontology).

The taxonomy has the topology of a causal network.

"Back propagation": Experiments labeled as "hot pain" are also labeled as "pain" experiments.

Is this set of coordinates consistent?

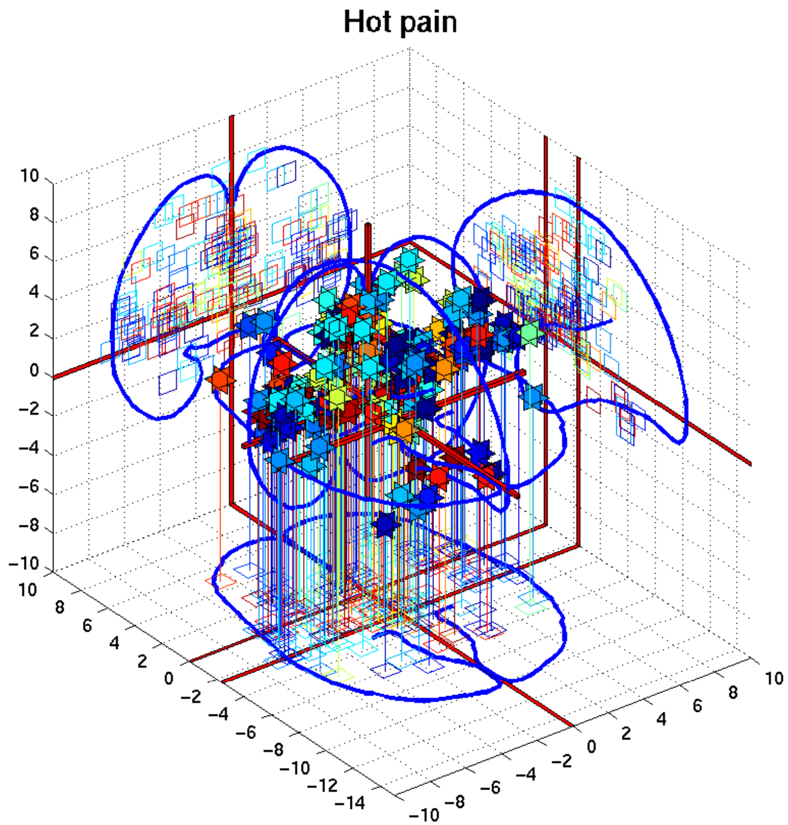

Figure 3: "Hot pain" Talairach coordinates. The different colors denote different experiments. The question is: Are they consistently positioned in Talairach space?

Voxelization of "external components"

The sets of Talairach coordinates are converted to a volume by kernel density estimation with a homogeneous Gaussian kernel (Nielsen and Hansen, 2002).

For one Talairach coordinate $\mathbf{v}_l$

$$p(\mathbf{v}|l) = (2\pi\sigma^2)^{-3/2} \exp\left[-\frac{(\mathbf{v}-\mathbf{v}_l)'(\mathbf{v}-\mathbf{v}_l)}{2\sigma^2}\right], \tag{1}$$

with the width σ fixed to 1 centimeter.

To form a resulting probability density volume $p(\mathbf{v}|t)$ for an external component t the individual components from each coordinate are multiplied by the appropriate priors and summed

$$p(\mathbf{v}|t) = \sum_{l,e} p(\mathbf{v}|l)\, P(l|e)\, P(e|t). \tag{2}$$

With priors chosen as

$$P(l|e) \propto \begin{cases} \frac{1}{\sqrt{|\mathcal{L}_e|}} \frac{1}{\sqrt{|\mathcal{E}_b|}} & \text{if } l \in \mathcal{L}_e \\ 0 & \text{otherwise,} \end{cases} \tag{3}$$

where $|\mathcal{L}_e|$ is the number of Talairach coordinates in the e experiment and $|\mathcal{E}_b|$ is the number of experiments in the paper it belongs to.

$$P(e|t) \propto \begin{cases} 1 & \text{if experiment } e \text{ is labeled as } t \\ 0 & \text{otherwise.} \end{cases} \tag{4}$$

The continuous volume is sampled at regular grid points to establish a vector $\mathbf{w}_t$ for each external component t

$$\mathbf{w}_t \equiv p(\mathbf{v}|t). \tag{5}$$

Permutation test statistic

$\mathbf{w}_r$: Volume generated from a sampling r among all experiments.

Maximum statistic u_r for the r resample (Holmes et al., 1996)

$$u_r(E) = \max_j [w_r(j)], \tag{6}$$

where j is an index over voxels and E is the number of experiments in the resample.

With R Monte Carlo resamplings we get a vector

$$\mathbf{u}(E) = [u_1(E) \ldots u_r(E) \ldots u_R(E)] \tag{7}$$

Distance to null-hypothesis $d_{t,j}$ for voxel j

$$d_{t,j} = \mathrm{Prob}\left[w_{t,j} > u(E_t)\right], \tag{8}$$

with E_t as the number of experiments for the external component t.

Results of permutation maximum statistic

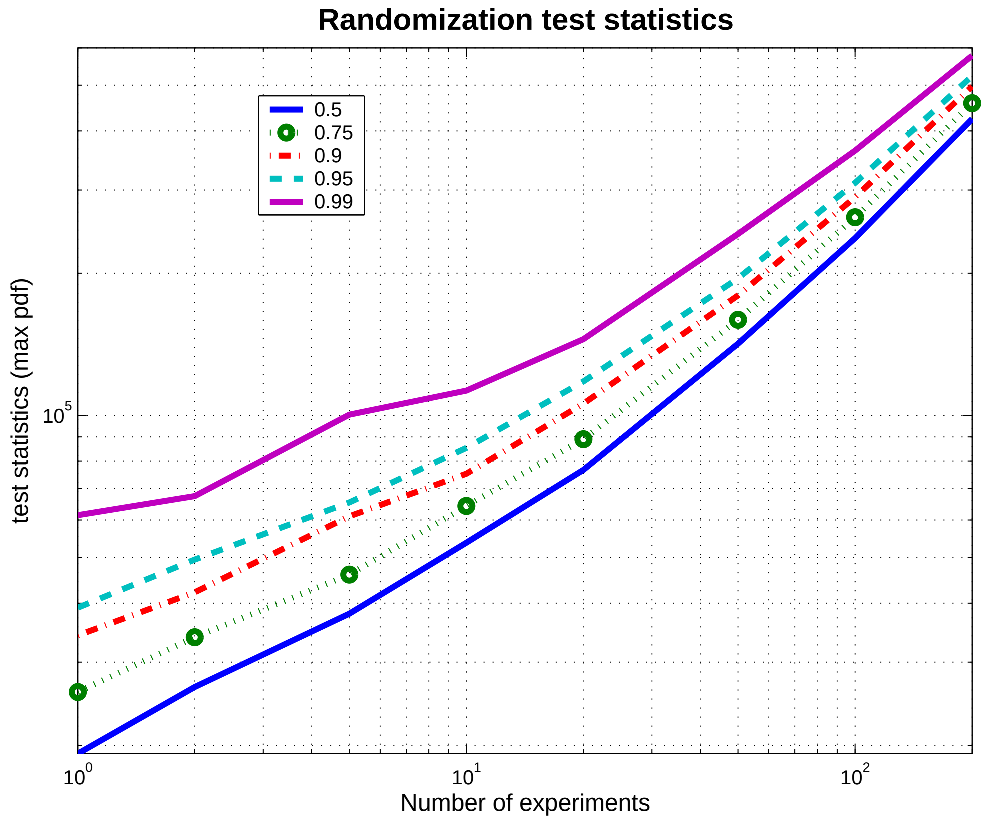

Figure 4: The test statistics at various distances to the null-hypothesis ($d = 1 - P$) after 3000 resamplings. The distance is shown as a function of the number of experiments E in the resampling.

Modeling the empirical distribution

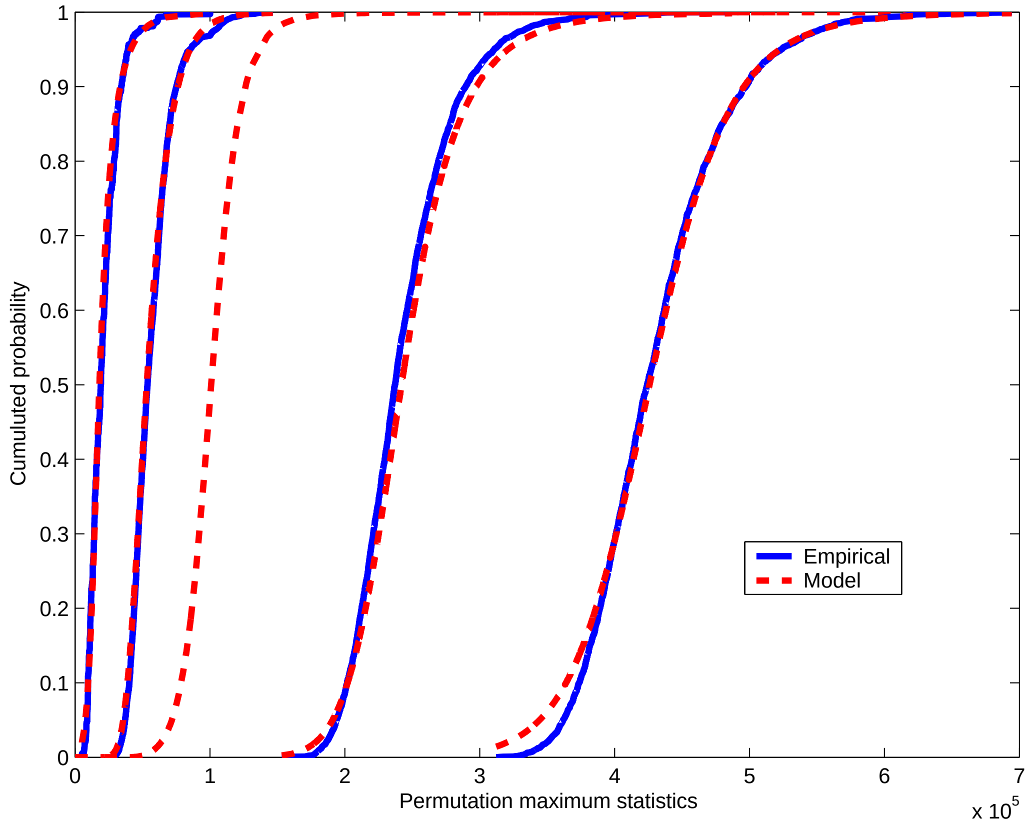

Figure 5: Empirical distribution and the distribution modeled with a two-layer feed-forward neural network targeting the function $f(E,u) = \text{atanh}(2d-1)$. Shown for varying number of experiments E.

Ranking of the most important results

#	d	x	y	z	Name (WOEXT)
1	1.00	0	−8	56	Localized movement (266)
2	1.00	0	−8	56	Motion, movement, locomotion (4)
3	1.00	56	−16	8	Disease (79)
4	1.00	0	0	40	Thermal pain (261)
5	1.00	0	0	40	Pain (40)
6	1.00	0	0	40	Temperature sensation (204)
7	1.00	0	−56	16	Memory (9)
8	1.00	0	0	40	Warm temperature sensation (207)
9	1.00	56	−16	0	Audition (14)
10	1.00	0	0	40	Somesthesis (17)
11	1.00	0	−56	16	Memory retrieval (24)
12	1.00	24	−8	−8	Unpleasantness (153)
13	1.00	56	−16	0	Voice (167)
14	0.99	24	−8	−8	Emotion (3)
15	0.99	−40	−72	8	Motion perception (132)

The top 15 elements of the list with the external components that score the highest, the distance to the null-hypothesis d, and the associated Talairach x, y and z coordinates.

The numbers in the parentheses are the Brede database identifiers for the external components (WOEXT).

This list was generated with coarse $8 \times 8 \times 8\text{mm}^3$ voxels and using the non-linear model approximation for the cumulative distribution functions.

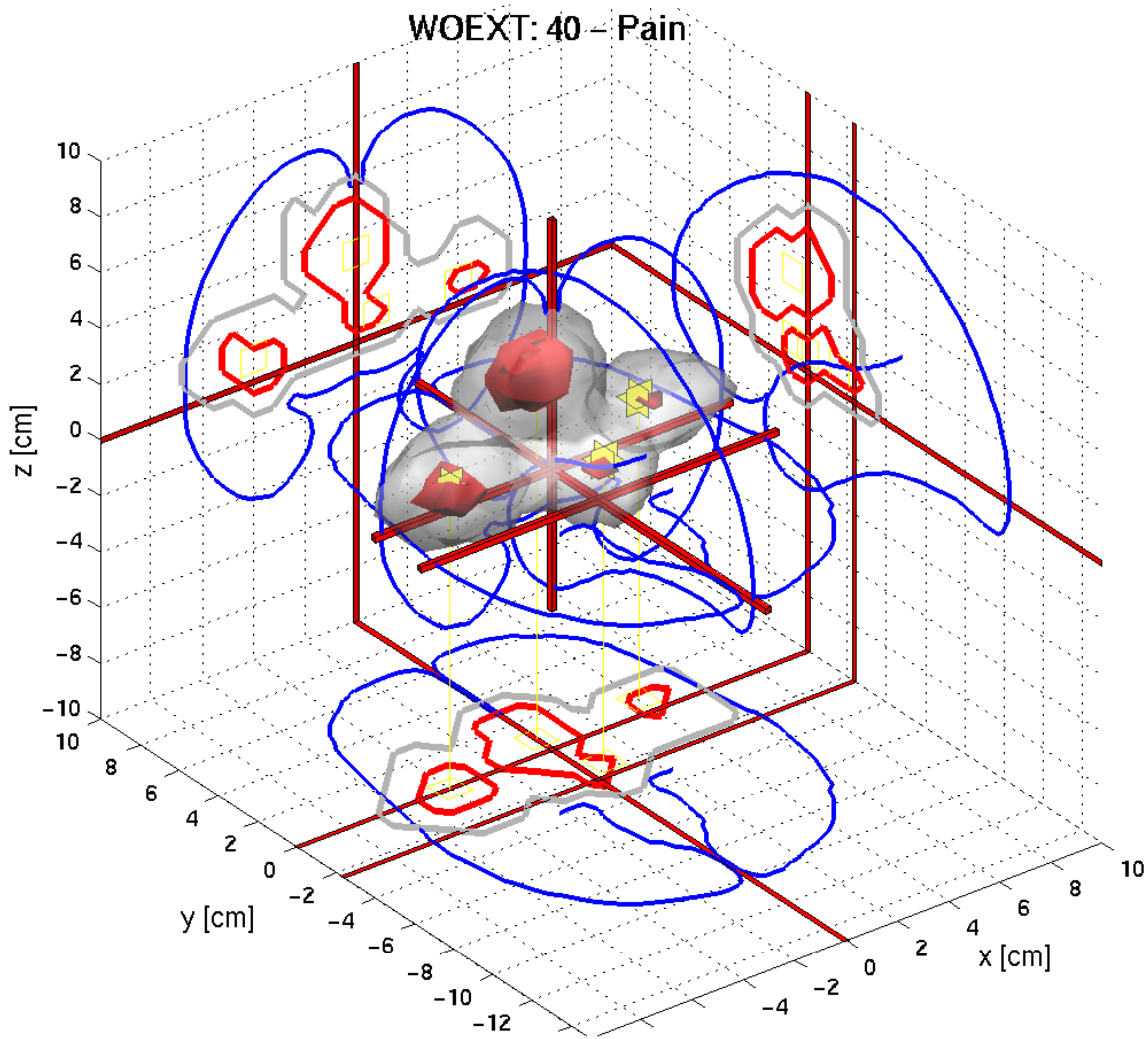
WOEXT: 40 – Pain
z [cm]
y [cm]
x [cm]
10
8
6
4
2
0
−2
−4
−6
−8
−10
−12

Plot of the important areas associated with the external component "pain".

The red opaque isosurface is on the level $d = 0.95$ in the distance volume while the gray transparent surface appears at $d = 0.05$.

Yellow glyphs appear at the local maxima in the thresholded volume. The viewpoint is situated nearest to the left superior posterior corner of the brain.

Interpretation: Four focal "brain activations" that appear in the figure are localized in areas (anterior cingulate, insula and thalamus) that an expert reviewer has previously identified as important in pain (Ingvar, 1999), thus there is consistency between our automated meta-analytic technique and a "manual" expert review.

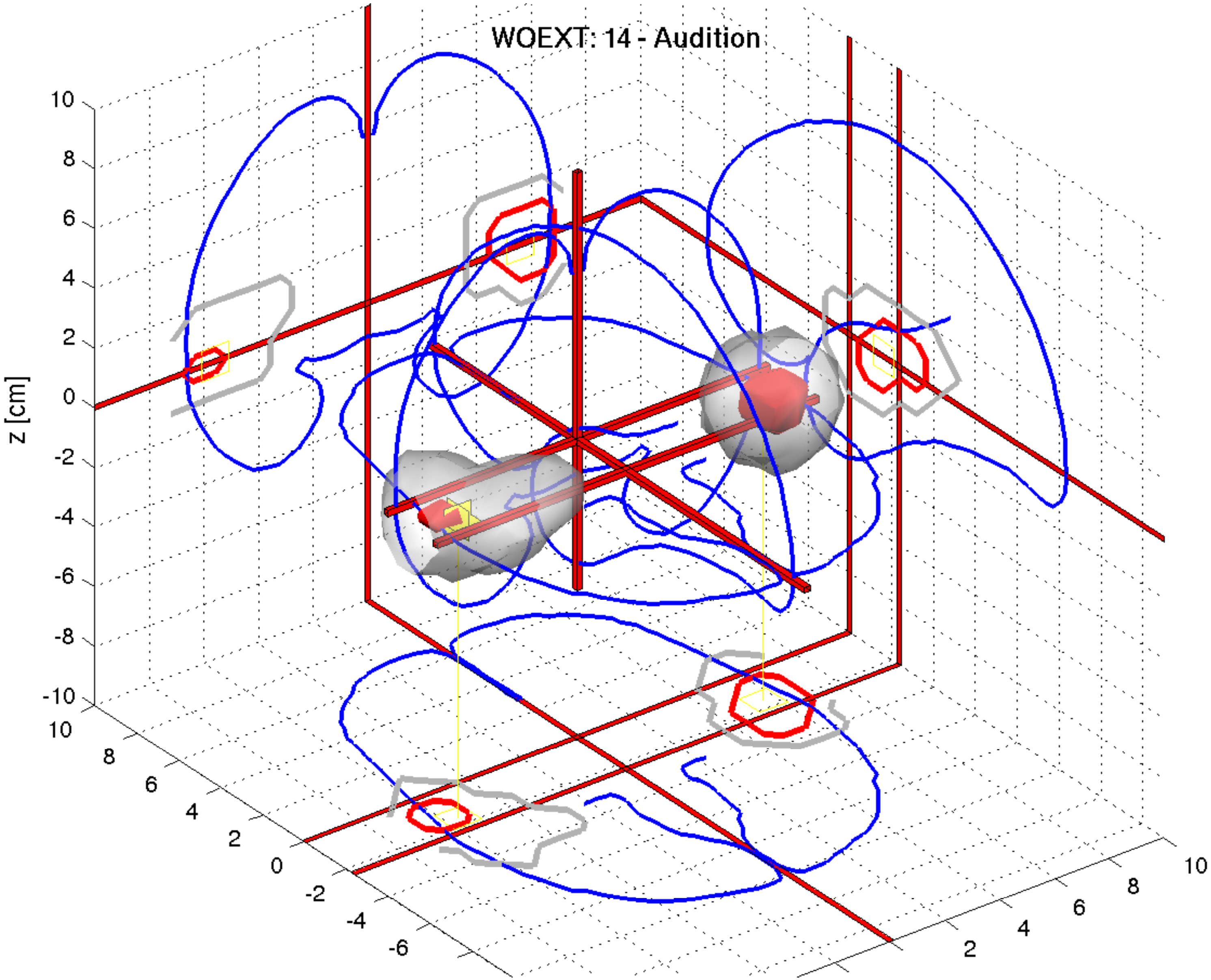
WOEXT: 14 - Audition
z [cm]
10
8
6
4
2
0
-2
-4
-6
-8
-10
10
8
6
4
2
0
-2
-4
-6
10
8
6
4
2

Functional labeling

Function labeling: Assign an external component (e.g., a brain function) to a Talairach coordinate.

Collect all distances in a (external component $\times$ voxel)-matrix $[\ d\ ]_{t,j} \equiv \mathbf{D}$.

For a given voxel (column in $\mathbf{D}$) sort the values and build a list with the most probable labels.

Example (Table 1) is a list generated for a coordinate in the posterior cingulate area $\mathbf{v} = (0, -56, 16)$.

It shows memory as a dominating theme in line with a "manual" review (Cabeza and Nyberg, 2000) and an automated review (Nielsen et al., 2004).

#	d	Name (WOEXT)
1	1.00	Memory (9)
2	1.00	Memory retrieval (24)
3	0.99	Episodic memory (49)
4	0.99	Long-term memory (112)
5	0.99	Declarative memory (319)
6	0.97	Association (457)
7	0.97	Associative Encoding (458)
8	0.97	Memory encoding (329)
9	0.97	Cognition (2)
10	0.96	Autobiographical memory (259)
11	0.94	Learning (33)
12	0.94	Episodic memory retrieval (109)
13	0.43	Disease (79)
14	0.16	Recognition (190)
15	0.14	Neurotic, stress and somatoform disorders (227)

Table 1: Example of a functional label list of a voxel $\mathbf{v} = (0, -56, 16)$ in the posterior cingulate area.

Summary

Data mining technique in a small neuroinformatics database.

Mining for consistent brain change across published human brain mapping studies.

Techniques: Construction of ontology, kernel density modeling, permutation maximum statistics.

Functional labeling also possible.

References

Balslev, D., Nielsen, F. Å., Paulson, O. B., and Law, I. (2004). Right temporoparietal cortex activation during visuo-proprioceptive conflict. *Cerebral Cortex*. PMID: 152384438. WOBIB: 128. Accepted.

Cabeza, R. and Nyberg, L. (2000). Imaging cognition II: An empirical review of 275 PET and fMRI studies. *Journal of Cognitive Neuroscience*, 12(1):1–47. PMID: 10769304. http://jocn.mitpress.org/cgi/content/abstract/12/1/1.

Holmes, A. P., Blair, R. C., Watson, J. D. G., and Ford, I. (1996). Non-parametric analysis of statistic images from functional mapping experiments. *Journal of Cerebral Blood Flow and Metabolism*, 16(1):7–22. PMID: 8530558.

Ingvar, M. (1999). Pain and functional imaging. *Philosophical Transactions of the Royal Society of London. Series B, Biological Sciences*, 354(1387):1347–1358. PMID: 10466155.

Nielsen, F. Å. (2003). The Brede database: a small database for functional neuroimaging. *NeuroImage*, 19(2). http://208.164.121.55/hbm2003/abstract/abstract906.htm. Presented at the 9th International Conference on Functional Mapping of the Human Brain, June 19–22, 2003, New York, NY. Available on CD-Rom.

Nielsen, F. Å., Balslev, D., and Hansen, L. K. (2004). Mining posterior cingulate. *NeuroImage*, 22. Presented at the 10th Annual Meeting of the Organization for Human Brain Mapping, June 14–17, 2004, Budapest, Hungary. Available on CD-ROM.

Nielsen, F. Å. and Hansen, L. K. (2002). Modeling of activation data in the BrainMap^{TM} database: Detection of outliers. *Human Brain Mapping*, 15(3):146–156. DOI: 10.1002/hbm.10012. http://www3.interscience.wiley.com/cgi-bin/abstract/89013001/. CiteSeer: http://citeseer.nj.nec.com/nielsen02modeling.html.

Talairach, J. and Tournoux, P. (1988). *Co-planar Stereotaxic Atlas of the Human Brain*. Thieme Medical Publisher Inc, New York. ISBN 0865772932.